EFFECTS OF PARABOLIC AND INVERTED PARABOLIC SALINITY GRADIENTS ON DOUBLE DIFFUSIVE MARANGONI CONVECTION IN A COMPOSITE LAYER AN EXACT STUDY

[1]R. Sumithra and [2]B. Komala

[1]Department of Mathematics, Government Science College, Bangalore – 560 001,
Karnataka, INDIA.

[2]Department of Mathematics, BTLITM, Bangalore-560 099,
Karnataka, INDIA.

ABSTRACT

The Effects of Parabolic and Inverted parabolic Salinity gradients on the onset of Double Diffusive Marangoni Convection in a two-layer system, comprising an incompressible two component fluid saturated porous layer over which lies a layer of the same fluid in the microgravity condition, are investigated. The upper boundary of the fluid layer is free and the lower boundary of the porous layer is rigid and both the boundaries are insulating to heat and mass. At the interface, the velocity, shear stress, normal stress, heat, heat flux, mass and mass flux are assumed to be continuous conducive for Darcy-Brinkman model. The resulting Eigen value problem is solved exactly. The Thermal Marangoni numbers for linear, parabolic and inverted parabolic salinity profiles are obtained. The effects of different physical parameters on the onset of double diffusive Marangoni convection are investigated for above profiles in detail.

Keywords: Double diffusive convection, Salinity gradients, Thermal Marangoni numbers, Darcy-Brinkman model

1. INTRODUCTION

In the generation of techno-savvy world, the chips made up of pure crystals are of great demand leading to the enormous scope for the evolutions and explorations in the industry of crystal growth. There are many methods of growing crystals and these can be classified on the basis of method of producing super saturation as Isothermal methods (constant temperature method) ex., Hydrothermal growth and Non isothermal methods (temperature variation method) In the case of Isothermal methods, any property of the crystal that is temperature dependent will be under better control. Hydrothermal growth is a crystal growth from aqueous solution at high temperature and pressure. Even under hydrothermal conditions most of the materials grown have very low solubilities in solvents. Thus to achieve reasonable solubilities, large quantities of other materials are added which do not react with the material being grown. These materials are called mineralizers. The apparatus consists of an autoclave consisting two layers. Nutrients in the lower part (nutrient region) of the autoclave dissolve in the fluid (solvent + Mineralizers + crystal material), which is kept to hotter than the upper part (growth region) of the autoclave. The temperature difference causes convection from the nutrient region to the growth region and the upper fluid is supercooled which drives the crystallization. Since the fluid has more than one diffusive component of different molecular diffusivities (heat, concentration of mineralizer) the convection is multi diffusive and the materials in the nutrient chips can be regarded as a porous medium. This method of growing crystals exactly simulates the double (if one mineralizer is added), triple (if two mineralizers are added) and multi component (if more than two mineralizers are added) diffusive convection in a horizontal composite layer(a fluid layer overlying a fluid saturated porous layer). In the case of non isothermal methods of growing crystals that is, when the temperature gradient is imposed on the system, the main advantage is that the diffusion path is usually shorter, so reasonable rates are achieved without elaborate control or apparatus investment. In these situations, maintaining a uniform temperature and salinity gradients is a limitation and occurrence of non-uniform temperature and salinity gradients is a reality. The study of non uniform gradients is not given much attention and the non uniform salinity gradients are rarely touched. Though some literature is available on the study of non uniform temperature gradients, but the non uniform salinity gradients is at scarce. Recently Subbarama Pranesh et al (2012) have investigated the effect of non uniform basic concentration gradient on the onset of double diffusive convection in a micropolar fluid layer heated and saluted from below and cooled from above. The Eigen values are obtained using Galerkian method for free-free, rigid-free, rigid-rigid velocity boundary combination with isothermal on spin-vanishing permeable boundaries. One linear and five non linear concentration profiles are considered and their comparative influence on onset is discussed and results are depicted graphically. It is observed that the fluid layer with suspended particles heated and saluted from below is more stable compared to the classical fluid layer without suspended particles. Here we make an attempt to study the effects of two non uniform salinity gradients (parabolic and inverted parabolic profile) on the onset of surface tension driven double diffusive convection in a horizontal composite layer by Exact method [6]. Here we give some literature on the effects of non uniform temperature gradients on Marangoni convection in single horizontal fluid and porous layers separately. Nanjundappa Rudraiah and Pradeep G Siddheshwar (2000) have investigated the effect of non-uniform basic temperature gradients on the onset of Marangoni convection in a horizontal layer of a Boussinesq fluid with suspended particles. It is observed that the fluid layer with suspended particles heated from below is more stable compared to the classical fluid layer without suspended particles. The problem has possible applications in microgravity situations [4]. Shivakumara et al (2002) have investigated the effect of different basic temperature gradients on the onset of ferro convection driven by combined surface tension and buoyancy forces are studied. The results indicate that the stability of Rayleigh-Bernard-Marangoni Ferro convection is significantly affected by basic temperature gradients and the mechanism for suppressing or augmenting the same is discussed in detail. It is shown that the results obtained under the limiting conditions compare well with the existing ones [1]. Melviana Johnson Fu et al (2009) have studied the effect of six different non-uniform basic state temperature gradients on the onsets of Marangoni convection in a horizontal micropolar fluid layer bounded below by a rigid plate and above by non-deformable free surface subjected to a constant heat flux. They used Rayleigh Ritz technique to solve the resulting Eigen value problem and discussed the influence of the various parameters on the onset of Marangoni convection [3]. Siti Suzillian Putri Mohamed Isa et al (2009) have investigated the effect of six different non-uniform basic temperature gradients on the onset of Marangoni convection in a horizontal layer with a free-slip bottom heated from below and cooled from above. They solved the resulting the Eigen value problem using single-term Galerkian expansion procedure and have discussed the effect of the various parameters on the onset of Marangoni convection [5]. Coming to the single porous layers, Shivakumara et al (2012) have investigated the effect of different forms of basic temperature gradients on the criterion for the onset of convection in a layer of an incompressible couple stress fluid saturated porous medium is investigated. It is shown that the principle of exchange of stability is valid, and the Eigen value problem is solved numerically using the Galerkian technique. The parabolic and inverted parabolic basic temperature profiles have the same effect on the onset of convection [2]. Sumithra and Manjunath (2014) have investigated the an exact study of Magneto-Marangoni-convection in a two layer system comprising an incompressible electrically conducting fluid saturated porous layer over which lies a layer of the same fluid in the presence of a vertical magnetic field in the microgravity condition. The lower rigid surface of the porous layer and the upper free surface are considered to be insulating to temperature perturbations. At the upper free surface, the surface tension effects depending on temperature are considered. At the interface, the normal and tangential components of velocity, heat and heat flux are assumed to be continuous. The resulting Eigen value problem is solved exactly for both parabolic and inverted parabolic temperature profiles and analytical expressions of the Thermal Marangoni Number are obtained. Effects of variation of different physical parameters on the Thermal Marangoni Number for both profiles are compared [7].

2. FORMULATION OF THE PROBLEM

We consider a horizontal two – component fluid saturated, isotropic, sparsely packed porous layer of thickness d_m underlying a two component fluid layer of thickness d , in the microgravity condition. The lower surface of the porous layer is rigid and the upper surface of the fluid layer is free with the surface tension effects depending on both temperature and concentration. Both the boundaries are kept at different constant temperatures and concentrations. A Cartesian coordinate system is chosen with the origin at the interface between porous and fluid layers and the z – axis, vertically upwards. The continuity, momentum, energy and concentration equations are,

$$\nabla \cdot \vec{q} = 0 \tag{1}$$

$$\rho_0 \left[\frac{\partial \vec{q}}{\partial t} + \left(\vec{q} \cdot \nabla \right) \vec{q} \right] = -\nabla P + \mu \nabla^2 \vec{q} \tag{2}$$

$$\frac{\partial T}{\partial t} + \left(\vec{q} \cdot \nabla \right) T = \kappa \nabla^2 T \tag{3}$$

$$\frac{\partial C}{\partial t} + \left(\vec{q} \cdot \nabla \right) C = \kappa_s \nabla^2 C \tag{4}$$

For the porous layer,

$$\nabla_m \cdot \vec{q}_m = 0 \tag{5}$$

$$\frac{\rho_0}{\phi}\left(\frac{\partial \vec{q}_m}{\partial t}\right) = -\nabla_m P_m + \mu_m \nabla^2 \vec{q}_m - \frac{\mu}{K}\vec{q}_m \quad (6)$$

$$A\frac{\partial T_m}{\partial t} + \left(\vec{q}_m \cdot \nabla_m\right)T_m = \kappa_m \nabla_m^2 T_m \quad (7)$$

$$\phi\frac{\partial C_m}{\partial t} + \left(\vec{q}_m . \nabla\right)C_m = \kappa_{sm}\nabla^2 C_m \quad (8)$$

Where the symbols in the above equations have the following meaning $\vec{q} = (u, v, w)$ is the velocity vector, t is the time, μ is the fluid viscosity, ρ_0 is the fluid density, $A = \frac{\left(\rho_0 C_p\right)_m}{\left(\rho C_p\right)_f}$ is the ratio of heat capacities, C_p is the specific heat, K is the permeability of the porous medium, T is the temperature, κ is the thermal diffusivity of the fluid, C is the concentration, κ_s is the solute diffusivity of the fluid, ϕ is the porosity, and the subscripts m and f refer to the porous medium and the fluid respectively. The basic steady state is assumed to be the quiescent and we consider the solution of the form,

$$\left[u, v, w, P, T, C\right] = \left[0, 0, 0, P_b(z), T_b(z), C_b(z)\right] \quad (9)$$

in the fluid layer
and in the porous layer

$$\left[u_m, v_m, w_m, P_m, T_m, C_m\right] = \left[0, 0, 0, P_{mb}(z_m), T_{mb}(z_m), C_{mb}(z_m)\right] \quad (10)$$

where the subscript ‘b’ denotes the basic state. The temperature distributions $T_b(z)$, $T_{mb}(z_m)$, are found to be

$$T_b(z) = T_0 + \frac{(T_u - T_0)z}{d} \text{ in } 0 \le z \le d \quad (11)$$

$$T_{mb}(z_m) = T_0 - \frac{(T_l - T_0)z_m}{d_m} \text{ in } 0 \le z_m \le d_m \quad (12)$$

$$T_0 = \frac{\kappa d_m T_u + \kappa_m d T_l}{\kappa d_m + \kappa_m d}$$ is the interface temperature.

The concentration distributions $C_b(z)$, $C_{mb}(z_m)$, are found to be

$$-\frac{\partial C_b}{\partial z} = \frac{C_0 - C_u}{d} h(z) \text{ in } 0 \le z \le d \quad (13)$$

$$-\frac{\partial C_{mb}}{\partial z_m} = \frac{C_L - C_0}{d_m} h_m(z_m) \text{ in } 0 \le z_m \le d_m \quad (14)$$

Here $h(z)$, $h_m(z_m)$ are salinity gradients in fluid and porous layers respectively such that $\int_0^d h(z)\,dz = d$ and $\int_0^{d_m} h_m(z_m)\,dz_m = d_m$. The subscript b denotes the basic state. At the interface $h(z) = h_m(z_m)$ and note that $C_0 = \frac{\kappa d_m C_u + \kappa_m d C_l}{\kappa d_m + \kappa_m d}$ is concentration at the interface.

In order to investigate the stability of the basic solution, infinitesimal disturbances are introduced in the form,

$$\left[\vec{q}, P, T, C\right] = \left[0, P_b(z), T_b(z), C_b(z)\right] + \left[\vec{q}', P', \theta, S\right] \quad (15)$$

And

$$\left[\vec{q}_m, P_m, T_m, C_m\right] = \left[0, P_{mb}(z_m), T_{mb}(z_m), C_{mb}(z_m)\right] + \left[\vec{q}_m', P_m', \theta_m, S_m\right] \quad (16)$$

where the primed quantities are the perturbed ones over their equilibrium counterparts. Now Equations (15) and (16) are substituted into the Equations (1) to (8) and are linearized in the usual manner. Next, the pressure term is eliminated from (2) and (6) by taking curl twice on these two equations and only the vertical component is retained.

The variables are then non-dimensionalized using d, $\frac{d^2}{\kappa}$, $\frac{\kappa}{d}$, $T_0 - T_u$ and $C_0 - C_u$ as the units of length, time velocity, temperature, and the concentration in the fluid layer and d_m, $\frac{d_m^2}{\kappa_m}$, $\frac{\kappa_m}{d_m}$, $T_l - T_0$, $C_l - C_0$ as the corresponding characteristic quantities in the porous layer. Note that the separate length scales are chosen for the two layers so that each layer is of unit depth.

In this manner the detailed flow fields in both the fluid and porous layers can be clearly obtained for all the depth ratios $\hat{d} = \frac{d_m}{d}$.

The dimensionless equations for the perturbed variables are given by,

$$\frac{1}{\Pr}\frac{\partial \nabla^2 w}{\partial t} = \nabla^4 w \tag{17}$$

$$\frac{\partial \theta}{\partial t} = w + \nabla^2 \theta \tag{18}$$

$$\frac{\partial S}{\partial t} = w\, h(z) + \tau\, \nabla^2 S \tag{19}$$

$$\frac{\beta^2}{\Pr_m}\frac{\partial \nabla_m^2 w_m}{\partial t} = \hat{\mu}\beta^2 \nabla_m^4 w_m - \nabla_m^2 w_m \tag{20}$$

$$A\frac{\partial \theta_m}{\partial t} = w_m + \nabla_m^2 \theta_m \tag{21}$$

$$\phi\frac{\partial S_m}{\partial t} = w_m\, h_m(z_m) + \tau_m \nabla_m^2 S_m \tag{22}$$

For the fluid layer $\Pr = \frac{\nu}{\kappa}$ is the Prandtl number, $\tau = \frac{\kappa_s}{\kappa}$ is the diffusivity ratio in the fluid layer. For the porous layer, $\Pr_m = \frac{\varepsilon \nu_m}{\kappa_m}$ is the Prandtl number, $\beta^2 = \frac{K}{d_m^2} = Da$ is the Darcy number, $\hat{\mu} = \frac{\nu_m}{\nu}$ is the viscosity ratio, $\tau_m = \frac{\kappa_{sm}}{\kappa_m}$ is the diffusivity ratio in the porous layer. We make the normal mode expansion and seek solutions for the dependent variables in the fluid and porous layers according to

$$\begin{bmatrix} w \\ \theta \\ S \end{bmatrix} = \begin{bmatrix} W(z) \\ \Theta(z) \\ S(z) \end{bmatrix} f(x, y) e^{nt} \tag{23}$$

And

$$\begin{bmatrix} w_m \\ \theta_m \\ S_m \end{bmatrix} = \begin{bmatrix} W_m(z_m) \\ \Theta_m(z_m) \\ S_m(z_m) \end{bmatrix} f(x_m, y_m) e^{n_m t} \tag{24}$$

With $\nabla_2^2 f + a^2 f = 0$ and $\nabla_{2m}^2 f_m + a_m^2 f_m = 0$, where a and a_m are the non-dimensional horizontal wave numbers, n and n_m are the frequencies. Since the dimensional horizontal wave numbers must be the same for the fluid and porous layers, we must have $\frac{a}{d} = \frac{a_m}{d_m}$ and hence $a_m = \hat{d}a$. Substituting Equations (23) and (24) into the Equations (17) to (22) and denoting the differential operator $\frac{\partial}{\partial z}$ and $\frac{\partial}{\partial z_m}$ by D and D_m respectively, an Eigen value problem consisting of the following ordinary differential equations, is obtained, In $0 \le z \le 1$,

$$\left(D^2 - a^2 + \frac{n}{\mathrm{Pr}}\right)\left(D^2 - a^2\right)W = 0 \quad (25)$$

$$\left(D^2 - a^2 + n\right)\Theta + W = 0 \quad (26)$$

$$\left[\tau\left(D^2 - a^2\right) + n\right]S + W\ h(z) = 0 \quad (27)$$

In $0 \le z_m \le 1$

$$\left[\left(D_m^2 - a_m^2\right)\hat{\mu}\beta^2 + \frac{n_m\beta^2}{\mathrm{Pr}_m} - 1\right]\left(D_m^2 - a_m^2\right)W_m = 0 \quad (28)$$

$$\left(D_m^2 - a_m^2 + n_m A\right)\Theta_m + W_m = 0 \quad (29)$$

$$\left[\tau_m\left(D_m^2 - a_m^2\right) + n_m\phi\right]S_m + W_m\ h_m(z_m) = 0 \quad (30)$$

It is known that the principle of exchange of instabilities holds for Double Diffusive Marangoni convection in both fluid and porous layers separately for certain choice of parameters. Therefore, we assume that the principle of exchange of instabilities holds even for the composite layers. In other words, it is assumed that the onset of convection is in the form of steady convection and accordingly, we take $n = n_m = 0$.

We get,

In $0 \le z \le 1$,

$$\left(D^2 - a^2\right)^2 W(z) = 0 \quad (31)$$

$$\left(D^2 - a^2\right)\Theta(z) + W(z) = 0 \quad (32)$$

$$\tau\left(D^2 - a^2\right)S(z) + W(z)\ h(z) = 0 \quad (33)$$

In $0 \le z_m \le 1$ $\left[\left(D_m^2 - a_m^2\right)\hat{\mu}\beta^2 - 1\right]\left(D_m^2 - a_m^2\right)W_m(z_m) = 0$ (34)

$$\left(D_m^2 - a_m^2\right)\Theta_m(z_m) + W_m(z_m) = 0 \quad (35)$$

$$\tau_m\left(D_m^2 - a_m^2\right)S_m(z_m) + W_m(z_m)h_m(z_m) = 0 \quad (36)$$

Thus to solve the above ordinary differential equation we need 16 boundary conditions.

3. BOUNDARY CONDITIONS

The bottom boundary is assumed to be rigid and insulating to temperature and concentration so the boundary conditions at $z_m = 0$ are

$$w_m = 0, \frac{\partial w_m}{\partial z_m} = 0, \frac{\partial T_m}{\partial z_m} = 0, \frac{\partial S_m}{\partial z_m} = 0 \quad (37)$$

The upper boundary is assumed to be free, insulating to temperature and concentration so the appropriate boundary conditions at $z = d$ are $w = 0,\quad \hat{\mu}\frac{\partial^2 w}{\partial z^2} = -\frac{\partial \sigma_t}{\partial T}\left[\nabla_2^2 T\right] - \frac{\partial \sigma_t}{\partial C}\left[\nabla_2^2 S\right],\quad \frac{\partial T}{\partial z} = 0, \frac{\partial S}{\partial z} = 0$ where $\sigma_t = \sigma_0 - \sigma_T\, T - \sigma_S\, S$ is the surface tension, here $\sigma_T = -\left(\frac{\partial \sigma_t}{\partial T}\right)_{T=T_0}$, $\sigma_S = -\left(\frac{\partial \sigma_t}{\partial S}\right)_{C=C_0}$ At the interface (i.e., at $z = 0, z_m = d_m$), the normal component of velocity, tangential velocity, temperature, heat flux, mass and mass flux are continuous and respectively yield (following Nield (1977)),

$$w = w_m,\quad \frac{\partial w}{\partial z} = \frac{\partial w_m}{\partial z_m},\quad T = T_m,\quad \kappa\frac{\partial T}{\partial z} = \kappa_m\frac{\partial T_m}{\partial z_m},\quad S = S_m,\quad \kappa\frac{\partial S}{\partial z} = \kappa_{sm}\frac{\partial S_m}{\partial z_m} \quad (38)$$

We note that two more velocity conditions are required at $z = 0$. Since we have used the Darcy-Brinkman equations of motion for the flow through the porous medium, the physically feasible boundary conditions on velocity are the following, at the interface $z = 0$ and $z_m = d_m$

$$P_m - 2\mu_m \frac{\partial w_m}{\partial z_m} = P - 2\mu \frac{\partial w}{\partial z} \qquad (39)$$

which will reduce to

$$\mu\left(3\nabla_2^2 + \frac{\partial^2}{\partial z^2}\right)\frac{\partial w}{\partial z} = -\frac{\mu_m}{K}\frac{\partial w_m}{\partial z_m} + \mu_m \beta^2\left(3\nabla_{2m}^2 + \frac{\partial^2}{\partial z_m^2}\right)\frac{\partial w_m}{\partial z_m}$$

The other appropriate velocity boundary condition at the interface $z = 0, z_m = d_m$ can be,

$$\mu\left(-\frac{\partial^2 w}{\partial z^2} + \nabla_2^2 w\right) = \mu_m\left(-\frac{\partial^2 w_m}{\partial z_m^2} + \nabla_{2m}^2 w_m\right) \qquad (40)$$

All the Sixteen boundary conditions (35) to (40) are non-dimensionalised and are subjected to Normal mode expansion and are given by

$$W(1) = 0, \quad D^2W(1) + M\, a^2\Theta(1) + M_s a^2 S(1) = 0, \quad D\Theta(1) = 0, \quad DS(1) = 0$$

$$\hat{T}W(0) = W_m(1), \quad \hat{T}\hat{d}DW(0) = D_m W_m(1), \quad \hat{T}\hat{d}^2\left(D^2 + a^2\right)W(0) = \hat{\mu}\left(D_m^2 + a_m^2\right)W_m(0)$$

$$\hat{T}\hat{d}^3\beta^2\left(D^3W(0) - 3a^2DW(0)\right) = -D_m W_m(1) + \hat{\mu}\beta^2\left(D_m^3 W_m(1) - 3a_m^2 D_m W_m(1)\right)$$

$$\Theta(0) = \hat{T}\Theta_m(1), \quad D\Theta(0) = D_m\Theta_m(1), \quad S(0) = \hat{S}S_m(1), \quad DS(0) = D_m S_m(1),$$

$$w_m(0) = 0, \quad D_m w_m(0) = 0, \quad D_m\Theta_m(0) = 0, \quad D_m S_m(0) = 0 \qquad (41)$$

Where $M = -\frac{\partial \sigma_t}{\partial T}\frac{(T_0 - T_u)d}{\nu\kappa}$ is the thermal Marangoni number, $M_s = -\frac{\partial \sigma_t}{\partial S}\frac{(C_0 - C_u)d}{\nu\kappa}$ is the solute Marangoni number, while $\hat{T} = (T_L - T_0)/(T_0 - T_U)$, $\hat{S} = (C_L - C_0)/(C_0 - C_U)$, and $\hat{d} = d_m / d$ is the depth ratio. We see that $\hat{\kappa} = \kappa_m / \kappa = \hat{d} / \hat{T}$ and $\hat{\kappa}_s = \kappa_{sm} / \kappa_s = \hat{d} / \hat{S}$ because the steady state heat and mass fluxes are continuous across the interface. The Equations (31) to (36) are to be solved with respect to the above boundary conditions (41).

4. EXACT SOLUTION

The solutions of the Equations (31) and (34) are independent of $\Theta(z)$, $S(z)$, $\Theta_m(z_m)$, $S_m(z_m)$ and thus can be solved and expressions for W and W_m can be obtained as,

$$W(z) = C_1 Cosh(az) + C_2 zCosh(az) + C_3 Sinh(az) + C_4 zSinh(az) \qquad (42)$$

$$W_m(z_m) = C_5 Cosh(a_m z_m) + C_6 Sinh(a_m z_m) + C_7 Cosh(\sigma z_m) + C_8 Sinh(\sigma z_m) \qquad (43)$$

where $\sigma = \sqrt{\frac{1}{\hat{\mu}a_m^2} + a_m^2}$, and the expressions for $W(z)$ and $W_m(z)$ are

$$W(z) = C_1\left[Cosh(az) + A_1 zCosh(az) + A_2 Sinh(az) + A_3 zSinh(az)\right] \qquad (44)$$

$$W_m(z_m) = C_1\left[A_4 Cosh(a_m z_m) + A_5 Sinh(a_m z_m) + A_6 Cosh(\sigma z_m) + A_7 Sinh(\sigma z_m)\right] \qquad (45)$$

where $A_1, A_2, A_3, A_4, A_5, A_6, A_7$ are constants which are determined using corresponding velocity the boundary conditions $(41)^1, (41)^5, (41)^6, (41)^7, (41)^8, (41)^{13}, (41)^{14}$ as

$$A_1 = A_4\Delta_3 + A_5\Delta_4, \quad A_2 = A_4\Delta_1 + A_5\Delta_2, \quad A_3 = -a + A_4\Delta_5 + A_5\Delta_6$$

$$A_4 = \frac{1}{\Delta_9}\left(\hat{T} - \frac{\Delta_{10}}{\Delta_8\Delta_9 - \Delta_{10}\Delta_7}\Big(\big(aSinh(a) - Cosh(a)\big)\Delta_9 - \hat{T}\Delta_7\Big)\right)$$

$$A_5 = \frac{\Big(\big(aSinh(a) - Cosh(a)\big)\Delta_9 - \hat{T}\Delta_7\Big)}{\Delta_8\Delta_9 - \Delta_{10}\Delta_7}, \quad A_6 = -A_4, \quad A_7 = \frac{-A_5 a_m}{\sigma}$$

And $\Delta_i^{'s}$ are

$$\Delta_1 = \frac{-1}{2a^3\hat{T}\hat{d}^3\beta^2}\Big[\big(-1 - 3a_m^2\hat{\mu}\beta^2\big)\big(a_m Sinh(a_m) - \sigma Sinh(\sigma)\big) + \hat{\mu}\beta^2\big(a_m^3 Sinh(a_m) - \sigma^3 Sinh(\sigma)\big)\Big]$$

$$\Delta_2 = \frac{-1}{2a^3\hat{T}\hat{d}^3\beta^2}\Big[\big(-1 - 3a_m^2\hat{\mu}\beta^2\big)\big(Cosh(a_m) - Cosh(\sigma)\big)a_m + \hat{\mu}\beta^2\big(a_m^2 Cosh(a_m) - \sigma^2 Cosh(\sigma)\big)a_m\Big]$$

$$\Delta_3 = \frac{1}{\hat{T}\hat{d}}\Big(a_m Sinh(a_m) - \sigma Sinh(\sigma) - \hat{T}\hat{d}a\Delta_1\Big), \Delta_4 = \frac{1}{\hat{T}\hat{d}}\Big(a_m(Cosh(a_m) - Cosh(\sigma)) - \hat{T}\hat{d}a\Delta_2\Big)$$

$$\Delta_5 = \frac{1}{2a\hat{T}\hat{d}^2}\Big[\hat{\mu}\Big(2a_m^2 Cosh(a_m) - \big(\sigma^2 + a_m^2\big)Cosh(\sigma)\Big)\Big]$$

$$\Delta_6 = \frac{1}{2a\hat{T}\hat{d}^2}\left[\hat{\mu}\left(2a_m^2 Sinh(a_m) - \frac{a_m}{\sigma}\big(\sigma^2 + a_m^2\big)Sinh(\sigma)\right)\right]$$

$$\Delta_7 = \Delta_3 Cosh(a) + \Delta_1 Sinh(a) + \Delta_5 Sinh(a), \Delta_8 = \Delta_4 Cosh(a) + \Delta_2 Sinh(a) + \Delta_6 Sinh(a)$$

$$\Delta_9 = Cosh(a_m) - Cosh(\sigma), \Delta_{10} = Sinh(a_m) - \frac{a_m}{\sigma}Sinh(\sigma)$$

The Temperature distributions are obtained from the Equations (32) and (35) by substituting expressions for W and W_m, are as below

$$\Theta(z) = C_1\{A_8 Cosh(az) + A_9 Sinh(az) - \frac{1}{4a}[Sinh(az)(2z + A_1 z^2 - \frac{A_3 z}{a}) + Cosh(az)(2A_2 z - \frac{A_1 z}{a} + A_3 z^2)]\}$$

$$\Theta_m(z_m) = C_1\{A_{10} Cosh(a_m z_m) + A_{11} Sinh(a_m z_m) - \frac{A_4 z_m}{2a_m} Sinh(a_m z_m) -$$

$$\frac{A_5 z_m}{2a_m} Cosh(a_m z_m) - \frac{A_6}{\sigma^2 - a_m^2} Cosh(\sigma z_m) - \frac{A_7}{\sigma^2 - a_m^2} Sinh(\sigma z_m)\}$$

The constants A_8, A_9, A_{10}, A_{11} are determined using temperature boundary conditions $(41)^3, (41)^9, (41)^{10}$, $(41)^{15}$ and are obtained as below.

$$A_8 = A_{10}\hat{T} Cosh(a_m) + \delta_4, \quad aA_9 = A_{10} a_m Sinh(a_m) + \delta_5$$

$$A_{10} = \frac{\delta_1 - a\delta_4 Sinh(a) - \delta_5 Cosh(a)}{\hat{T}aCosh(a_m)Sinh(a) + a_m Cosh(a)Sinh(a_m)}, \quad A_{11} = \frac{1}{a_m}\left(\frac{A_5}{2a_m} + \frac{A_7\sigma}{\sigma^2 - a_m^2}\right)$$

Where $\delta_i^{'s}$ are

$$\delta_1 = \frac{1}{4a}\left[aCosh(a)\left(2 + A_1 - \frac{A_3}{a}\right) + Sinh(a)\left(2 + 2A_1 - \frac{A_3}{a}\right)\right]$$
$$+\frac{1}{4a}\left[aSinh(a)\left(2A_2 - \frac{A_1}{a} + A_3\right) + Cosh(a)\left(2A_2 - \frac{A_1}{a} + 2A_3\right)\right]$$
$$\delta_2 = \frac{A_4}{2a_m}Sinh(a_m) + \frac{A_5}{2a_m}Cosh(a_m) + \frac{A_6}{\sigma^2 - a_m^2}Cosh(\sigma) + \frac{A_7}{\sigma^2 - a_m^2}Sinh(\sigma)$$
$$\delta_3 = \frac{A_4}{2a_m}\left(Sinh(a_m) + a_mCosh(a_m)\right) + \frac{A_5}{2a_m}\left(Cosh(a_m) + a_mSinh(a_m)\right) + \frac{A_6\sigma}{\sigma^2 - a_m^2}Sinh(\sigma) + \frac{A_7\sigma}{\sigma^2 - a_m^2}Cosh(\sigma)$$
$$\delta_4 = \frac{1}{a_m}\left(\frac{A_5}{2a_m} + \frac{A_7\sigma}{\sigma^2 - a_m^2}\right)\hat{T}Sinh(a_m) - \hat{T}\delta_2$$
$$\delta_5 = \frac{1}{4a}\left(2A_2 - \frac{A_1}{a}\right) + \left(\frac{A_5}{2a_m} + \frac{A_7\sigma}{\sigma^2 - a_m^2}\right)Cosh(a_m) - \delta_3$$

4.1 Linear Salinity Profile

We consider linear salinity profile of the form $h(z) = h_m(z_m) = 1$, substituting this in eq.(33) and (36) the expressions for $S(z)$ and $S_m(z_m)$ are obtained as

$$S(z) = C_1\left\{A_{12}Cosh(az) + A_{13}Sinh(az) - \frac{1}{4a\tau}\left[Sinh(az)\left(2z + A_1z^2 - \frac{A_3z}{a}\right) + Cosh(az)\left(2A_2z - \frac{A_1z}{a} + A_3z^2\right)\right]\right\}$$

$$S_m(z_m) = C_1\left\{A_{14}Cosh(a_mz_m) + A_{15}Sinh(a_mz_m) - \right.$$
$$\left.\frac{1}{\tau_{pm}}\left(\frac{A_4z_m}{2a_m}Sinh(a_mz_m) + \frac{A_5z_m}{2a_m}Cosh(a_mz_m) + \frac{A_6}{\sigma^2 - a_m^2}Cosh(\sigma z_m) + \frac{A_7}{\sigma^2 - a_m^2}Sinh(\sigma z_m)\right)\right\}$$

The constants $A_{12}, A_{13}, A_{14}, A_{15}$ are determined using salinity boundary conditions $(41)^4, (41)^{11}, (41)^{12}, (41)^{16}$ and are obtained as below.

$$A_{12} = \hat{S}\left[\frac{\delta_6 - \delta_{10}}{\delta_9}Cosh(a_m) + \frac{Sinh(a_m)}{a_m\tau_{pm}}\left(\frac{A_5}{2a_m} + \frac{A_7\sigma}{\sigma^2 - a_m^2}\right) - \delta_7\right]$$
$$aA_{13} = \left[\frac{\delta_6 - \delta_{10}}{\delta_9}a_mSinh(a_m) + \frac{Cosh(a_m)}{\tau_{pm}}\left(\frac{A_5}{2a_m} + \frac{A_7\sigma}{\sigma^2 - a_m^2}\right) + \delta_3\right], \quad A_{14} = \frac{\delta_6 - \delta_{10}}{\delta_9}, \quad A_{15} = \frac{1}{a_m\tau_{pm}}\left(\frac{A_5}{2a_m} + \frac{A_7\sigma}{\sigma^2 - a_m^2}\right)$$

Where $\delta_i^{'s}$, for i = 6 to 10 are

$$\delta_6 = \frac{1}{4a\tau}\left[Sinh(a)\left(2 + 2A_1 - \frac{A_3}{a}\right) + aCosh(a)\left(2 + A_1 - \frac{A_3}{a}\right) + \right.$$
$$\left.Cosh(a)\left(2A_2 + 2A_3 - \frac{A_1}{a}\right) + aSinh(a)\left(2A_2 + A_3 - \frac{A_1}{a}\right)\right]$$

$$\delta_7 = \frac{1}{\tau_{pm}}\left[\frac{A_4}{2a_m}Sinh(a_m) + \frac{A_5}{2a_m}Cosh(a_m) + \frac{A_6}{\sigma^2 - a_m^2}Cosh(\sigma) + \frac{A_7}{\sigma^2 - a_m^2}Sinh(\sigma)\right]$$

$$\delta_8 = \frac{1}{4a\tau}\left(2A_2 - \frac{A_1}{a}\right) - \frac{1}{\tau_{pm}}\left[\frac{A_4}{2a_m}Sinh(a_m) + \frac{A_4}{2}Cosh(a_m) + \frac{A_5}{2a_m}Cosh(a_m) + \frac{A_5}{2}Sinh(a_m)\right.$$

$$\left.\frac{A_6\sigma}{\sigma^2 - a_m^2}Sinh(\sigma) + \frac{A_7\sigma}{\sigma^2 - a_m^2}Cosh(\sigma)\right]$$

$$\delta_9 = a\hat{S}Sinh(a)Cosh(a_m) + a_m Cosh(a)Sinh(a_m)$$

$$\delta_{10} = \frac{a\hat{S}Sinh(a)Sinh(a_m)}{a_m\tau_{pm}}\left(\frac{A_5}{2a_m} + \frac{A_7\sigma}{\sigma^2 - a_m^2}\right) - \hat{S}aSinh(a)\delta_7 +$$

$$\frac{Cosh(a)Cosh(a_m)}{\tau_{pm}}\left(\frac{A_5}{2a_m} + \frac{A_7\sigma}{\sigma^2 - a_m^2}\right) + \delta_8 Cosh(a)$$

The Thermal Marangoni number for Linear Salinity Profile is obtained by the boundary condition $(41)^2$ as

$$M_t = \frac{-\left(\Delta_{11} + M_s a^2 \Delta_{12}\right)}{a^2\Delta_{13}}$$

Where

$$\Delta_{11} = C_1\left[a^2Cosh(a) + A_1\left(2aSinh(a) + a^2Cosh(a)\right) + A_2a^2Sinh(a) + A_3\left(2aCosh(a) + a^2Sinh(a)\right)\right]$$

$$\Delta_{12} = C_1\left\{A_{12}Cosh(a) + A_{13}Sinh(a) - \frac{1}{4a\tau}\left[Sinh(a)\left(2 + A_1 - \frac{A_3}{a}\right) + Cosh(a)\left(2A_2 - \frac{A_1}{a} + A_3\right)\right]\right\}$$

$$\Delta_{13} = C_1\{A_8Cosh(a) + A_9Sinh(a) - \frac{1}{4a}[Sinh(a)(2 + A_1 - \frac{A_3}{a}) + Cosh(a)(2A_2 - \frac{A_1}{a} + A_3)]\}$$

4.2 Parabolic Salinity Profile

We consider parabolic salinity profile of the form $h(z) = 2z, h_m(z_m) = 2z_m$, substituting this in eq.(33) and (36), the expressions for $S(z)$ and $S_m(z_m)$ are obtained as

$$S(z) = C_1\left\{A_{16}Cosh(az) + A_{17}Sinh(az) - \frac{2}{\tau}\left[Sinh(az)\left(\frac{z^2}{4a} + \frac{A_1z^3}{12a} + \frac{A_1z}{4a^3} - \frac{A_2z}{4a^2} - \frac{A_3z^2}{4a^2}\right)\right.\right.$$

$$\left.\left.+Cosh(az)\left(-\frac{z}{4a^2} - \frac{A_1z^2}{4a^2} + \frac{A_2z^2}{4a} + \frac{A_3z^3}{12a} + \frac{A_3z}{4a^3}\right)\right]\right\}$$

$$S_m(z_m) = C_1\left\{A_{18}Cosh(a_mz_m) + A_{19}Sinh(a_mz_m) - \frac{2}{\tau_{pm}}\left(Sinh(a_mz_m)\left(\frac{A_4z_m^2}{4a_m} - \frac{A_5z_m}{4a_m^2}\right) + Cosh(a_mz_m)\left(\frac{A_5z_m^2}{4a_m} - \frac{A_4z_m}{4a_m^2}\right)\right.\right.$$

$$\left.\left.+Cosh(\sigma z_m)\left(\frac{A_6z_m}{\sigma^2 - a_m^2} - \frac{2\sigma A_7}{\left(\sigma^2 - a_m^2\right)^2}\right) + Sinh(\sigma z_m)\left(\frac{A_7z_m}{\sigma^2 - a_m^2} - \frac{2\sigma A_6}{\left(\sigma^2 - a_m^2\right)^2}\right)\right)\right\}$$

The constants $A_{16}, A_{17}, A_{18}, A_{19}$ are determined using the salinity boundary conditions $(41)^4, (41)^{11}, (41)^{12}$, $(41)^{16}$ and are obtained as below.

$$A_{16}=\hat{S}\left[\frac{p_7}{p_8}Cosh(a_m)+\frac{p_7}{a_m}Sinh(a_m)-p_3\right]\quad ,aA_{17}=\frac{p_7}{p_8}a_mSinh(a_m)+p_5Cosh(a_m)-p_6,$$

$$A_{18}=\frac{p_7}{p_8},\quad a_mA_{19}=p_5$$

Where $p_i^{'s}$, for i = 1 to 8 are

$$p_1=\frac{2}{\tau}\left(\frac{-1}{4a^2}+\frac{A_3}{4a^3}\right)$$

$$p_2=\frac{2}{\tau}\left[Sinh(a)\left(\frac{1}{2a}+\frac{A_1}{4a}+\frac{A_1}{4a^3}-\frac{A_2}{4a^2}-\frac{A_3}{2a^2}\right)+aCosh(a)\left(\frac{1}{4a}+\frac{A_1}{12a}+\frac{A_1}{4a^3}-\frac{A_2}{4a^2}-\frac{A_3}{4a^2}\right)\right.$$

$$Cosh(a)\left(\frac{-1}{4a^2}-\frac{A_1}{2a^2}+\frac{A_2}{2a}+\frac{A_3}{4a}+\frac{A_3}{4a^3}\right)+aSinh(a)\left(\frac{-1}{4a^2}-\frac{A_1}{4a^2}+\frac{A_2}{4a}+\frac{A_3}{12a}+\frac{A_3}{4a^3}\right)$$

$$p_3=\frac{2}{\tau_{pm}}\left(Sinh(a_m)\left(\frac{A_4}{4a_m}-\frac{A_5}{4a_m^2}\right)+Cosh(a_m)\left(\frac{A_5}{4a_m}-\frac{A_4}{4a_m^2}\right)\right.$$

$$\left.+Cosh(\sigma)\left(\frac{A_6}{\sigma^2-a_m^2}-\frac{2\sigma A_7}{\left(\sigma^2-a_m^2\right)^2}\right)+Sinh(\sigma)\left(\frac{A_7}{\sigma^2-a_m^2}-\frac{2\sigma A_6}{\left(\sigma^2-a_m^2\right)^2}\right)\right\}$$

$$p_4=\frac{2}{\tau_{pm}}\left(a_mCosh(a_m)\left(\frac{A_4}{4a_m}-\frac{A_5}{4a_m^2}\right)+Sinh(a_m)\left(\frac{A_4}{2a_m}-\frac{A_5}{4a_m^2}\right)+a_mSinh(a_m)\left(\frac{A_5}{4a_m}-\frac{A_4}{4a_m^2}\right)\right.$$

$$+Cosh(a_m)\left(\frac{A_5}{2a_m}-\frac{A_4}{4a_m^2}\right)+\sigma Cosh(\sigma)\left(\frac{A_7}{\sigma^2-a_m^2}-\frac{2\sigma A_6}{\left(\sigma^2-a_m^2\right)^2}\right)+Sinh(\sigma)\left(\frac{A_7}{\sigma^2-a_m^2}\right)$$

$$+\sigma Sinh(\sigma)\left(\frac{A_6}{\sigma^2-a_m^2}-\frac{2\sigma A_7}{\left(\sigma^2-a_m^2\right)^2}\right)+Cosh(\sigma)\left(\frac{A_6}{\sigma^2-a_m^2}\right)$$

$$p_5=\frac{2}{\tau_{pm}}\left(-\frac{A_4}{4a_m^2}+\sigma\left(\frac{-2\sigma A_6}{\left(\sigma^2-a_m^2\right)^2}\right)+\frac{A_6}{\sigma^2-a_m^2}\right),\quad p_6=p_4-p_1$$

$$p_7=p_2+p_6Cosh(a)-p_5Cosh(a_m)Cosh(a)+p_3\hat{S}aSinh(a)-\frac{p_5}{a_m}\hat{S}aSinh(a)Sinh(a_m)$$

$$p_8=\hat{S}aSinh(a)Cosh(a_m)+aCosh(a)Sinh(a_m)$$

The Thermal Marangoni number for Parabolic Salinity Profile is obtained by the boundary condition $(41)^2$ as

$$M_t=\frac{-\left(\Delta_{11}+M_sa^2\Delta_{12}\right)}{a^2\Delta_{13}}$$

Where

$$\Delta_{11}=C_1\left[a^2Cosh(a)+A_1\left(2aSinh(a)+a^2Cosh(a)\right)+A_2a^2Sinh(a)+A_3\left(2aCosh(a)+a^2Sinh(a)\right)\right]$$

$$\Delta_{12}=C_1\left\{A_{16}Cosh(a)+A_{17}Sinh(a)-\right.$$

$$\frac{2}{\tau}\left[Sinh(a)\left(\frac{1}{4a}+\frac{A_1}{12a}+\frac{A_1}{4a^3}-\frac{A_2}{4a^2}-\frac{A_3}{4a^2}\right)+Cosh(a)\left(-\frac{1}{4a^2}-\frac{A_1}{4a^2}+\frac{A_2}{4a}+\frac{A_3}{12a}+\frac{A_3}{4a^3}\right)\right]\Bigg\}$$

$$\Delta_{13}=C_1\{A_8Cosh(a)+A_9Sinh(a)-\frac{1}{4a}[Sinh(a)(2+A_1-\frac{A_3}{a})+Cosh(a)(2A_2-\frac{A_1}{a}+A_3)]\}$$

4.3 Inverted Parabolic Salinity Profile

We consider parabolic salinity profile of the form $h(z)=2(1-z), h_m(z_m)=2(1-z_m)$, substituting this in eq.(33) and (36) the expressions for $S(z)$ and $S_m(z_m)$ are obtained as

$$S(z)=C_1\Bigg\{A_{20}Cosh(az)+A_{21}Sinh(az)+\frac{2}{\tau}\Bigg(Sinh(az)\left(\frac{-2z-A_1z^2+z^2}{4a}+\frac{A_1z^3}{12a}+\frac{A_1z}{4a^3}+\frac{A_3z-A_2z-A_3z^2}{4a^2}\right)+$$

$$Cosh(az)\left(\frac{-2A_2z-A_3z^2+A_2z^2}{4a}+\frac{A_3z^2}{12a}+\frac{A_3z}{4a^3}+\frac{A_1z-z-A_1z^2}{4a^2}\right)\Bigg)\Bigg\}$$

$$S_m(z_m)=C_1\Big\{A_{22}Cosh(a_mz_m)+A_{23}Sinh(a_mz_m)+$$

$$\frac{2}{\tau_{pm}}\Bigg(Sinh(a_mz_m)\left(\frac{-A_4z_m}{2a_m}+\frac{A_4z_m^2}{4a_m}-\frac{A_5z_m}{4a_m^2}\right)+Cosh(a_mz_m)\left(\frac{-A_5z_m}{2a_m}+\frac{A_5z_m^2}{4a_m}-\frac{A_4z_m}{4a_m^2}\right)$$

$$+Cosh(\sigma z_m)\left(\frac{-A_6}{\sigma^2-a_m^2}+\frac{A_6z_m}{\sigma^2-a_m^2}-\frac{2\sigma A_7}{\left(\sigma^2-a_m^2\right)^2}\right)+Sinh(\sigma z_m)\left(\frac{-A_7}{\sigma^2-a_m^2}+\frac{A_7z_m}{\sigma^2-a_m^2}-\frac{2\sigma A_6}{\left(\sigma^2-a_m^2\right)^2}\right)\Bigg)\Bigg\}$$

The constants $A_{20}, A_{21}, A_{22}, A_{23}$ are determined using salinity boundary conditions $(41)^4, (41)^{11}, (41)^{12}, (41)^{16}$ and are obtained as below.

$$A_{20}=\hat{S}\left[A_{22}Cosh(a_m)-\frac{I_5}{a_m}Sinh(a_m)+I_3\right],\quad aA_{21}=A_{22}a_mSinh(a_m)-I_5Cosh(a_m)-I_1+I_4$$

$$A_{22}=\frac{I_6}{I_7},\qquad a_mA_{23}=-I_5$$

Where $I_i^{'s}$, for $i=1 to 7$ are

$$I_1=\frac{2}{\tau}\left(\frac{-1}{4a^2}+\frac{A_3}{4a^3}-\frac{2A_2}{4a}+\frac{A_1}{4a^2}\right)$$

$$I_2=\frac{2}{\tau}\Bigg[Sinh(a)\left(-\frac{2A_1}{4a}+\frac{A_1}{4a^3}-\frac{A_2+A_3}{4a^2}+\frac{A_1}{4a}\right)+aCosh(a)\left(\frac{-1-A_1}{4a}+\frac{A_1}{12a}+\frac{A_1}{4a^3}-\frac{A_2}{4a^2}\right)$$

$$Cosh(a)\left(-\frac{A_1+1}{4a^2}-\frac{2A_3}{4a}+\frac{2A_3}{12a}+\frac{A_3}{4a^3}\right)+aSinh(a)\left(-\frac{A_2+A_3}{4a}-\frac{1}{4a^2}+\frac{A_3}{12a}+\frac{A_3}{4a^3}\right)$$

$$I_3=\frac{2}{\tau_{pm}}\Bigg(Sinh(a_m)\left(-\frac{A_4}{4a_m}-\frac{A_5}{4a_m^2}\right)+Cosh(a_m)\left(-\frac{A_5}{4a_m}-\frac{A_4}{4a_m^2}\right)$$

$$+Cosh(\sigma)\left(-\frac{2\sigma A_7}{\left(\sigma^2-a_m^2\right)^2}\right)+Sinh(\sigma)\left(-\frac{2\sigma A_6}{\left(\sigma^2-a_m^2\right)^2}\right)\Bigg)$$

$$I_4=\frac{2}{\tau_{pm}}\left(a_m Cosh(a_m)\left(-\frac{A_4}{4a_m}-\frac{A_5}{4a_m^2}\right)+Sinh(a_m)\left(-\frac{A_5}{4a_m^2}\right)+\right.$$

$$\left.\sigma Cosh(\sigma)\left(-\frac{2\sigma A_6}{\left(\sigma^2-a_m^2\right)^2}\right)+Sinh(\sigma)\left(\frac{A_7}{\sigma^2-a_m^2}\right)+\sigma Sinh(\sigma)\left(-\frac{2\sigma A_7}{\left(\sigma^2-a_m^2\right)^2}\right)+Cosh(\sigma)\left(\frac{A_6}{\sigma^2-a_m^2}\right)\right)$$

$$I_5=\frac{2}{\tau_{pm}}\left(-\frac{A_5}{2a_m}-\frac{A_4}{4a_m^2}+\sigma\left(\frac{-A_7}{\sigma^2-a_m^2}+\frac{-2\sigma A_6}{\left(\sigma^2-a_m^2\right)^2}\right)+\frac{A_6}{\sigma^2-a_m^2}\right)$$

$$I_6=-I_2-I_4Cosh(a)+I_5Cosh(a_m)Cosh(a)-I_3\hat{S}aSinh(a)+\frac{I_5}{a_m}\hat{S}aSinh(a)Sinh(a_m)+I_1Cosh(a)$$

$$I_7=\hat{S}aSinh(a)Cosh(a_m)+a_mCosh(a)Sinh(a_m)$$

The Thermal Marangoni number for inverted Parabolic Salinity Profile is obtained by the boundary condition $(41)^2$ as

$$M_t=\frac{-\left(\Delta_{11}+M_s a^2\Delta_{12}\right)}{a^2\Delta_{13}}$$

Where

$$\Delta_{11}=C_1\left[a^2Cosh(a)+A_1\left(2aSinh(a)+a^2Cosh(a)\right)+A_2a^2Sinh(a)+A_3\left(2aCosh(a)+a^2Sinh(a)\right)\right]$$

$$\Delta_{12}=C_1\left\{A_{20}Cosh(a)+A_{21}Sinh(a)+\frac{2}{\tau}\left(Sinh(a)\left(\frac{-1-A_1}{4a}+\frac{A_1}{12a}+\frac{A_1}{4a^3}-\frac{A_2}{4a^2}\right)+\right.\right.$$

$$\left.\left.Cosh(a)\left(\frac{-A_2-A_3}{4a}+\frac{A_3}{12a}+\frac{A_3}{4a^3}-\frac{1}{4a^2}\right)\right)\right\}$$

$$\Delta_{13}=C_1\{A_8Cosh(a)+A_9Sinh(a)-\frac{1}{4a}[Sinh(a)(2+A_1-\frac{A_3}{a})+Cosh(a)(2A_2-\frac{A_1}{a}+A_3)]\}$$

5. INTERPRETATIONS

The Thermal Marangoni numbers for the profiles, namely, linear, parabolic and inverted parabolic profiles for different parameters are presented graphically as a function of depth ratio $\hat{d}$ by fixing the other parameters. The effects of the variations of the parameters like Horizontal Wave number a, Viscosity ratio $\hat{\mu}=\frac{\mu_m}{\mu}$, Solute Marangoni number M_s, Diffusivity ratio τ, and the Darcy number Da on the thermal Marangoni number is displayed in figures 2, 3, 4, 5 and 6.

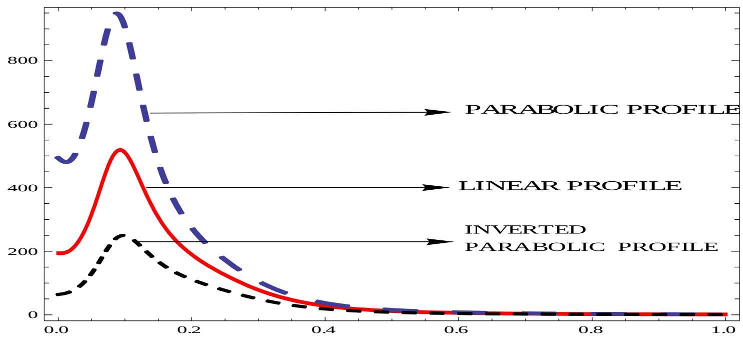

Fig.1: The variation of thermal Marangoni number for Linear, Parabolic and Inverted parabolic profiles with respect to the depth ratio. Figure1 shows the variation of thermal Marangoni numbers for different profiles with respect to the

depth ratio for fixed values of $Da = 10, \hat{S} = 1, \hat{T} = 1, \tau = 1, \tau_{pm} = 1, a = 5, M_s = 10, \mu = 5.$ Here the thermal Marangoni numbers for the profiles differ only for smaller values of depth ratios. Graphically it is evident that the parabolic salinity profile is the most stable one and the inverted salinity profile is the unstable one, so by choosing the appropriate salinity profile one can control the onset of double diffusive Marangoni convection in a composite layer in microgravity condition.

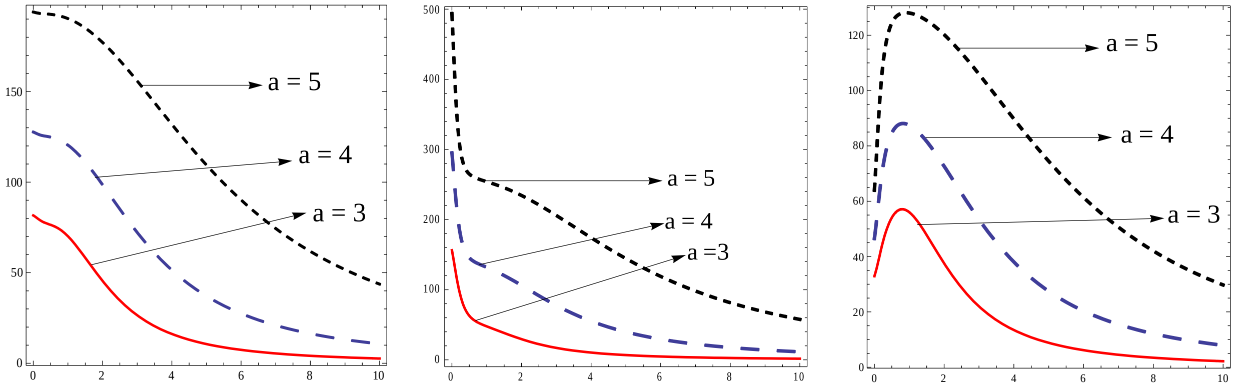

Fig. **(a)** Fig **(b)** Fig. **(c)**

Fig 2. The effects of horizontal wave number $a = 3, 4, 5$ on the Thermal Marangoni numbers M_t

The effects of $'a'$ horizontal wave number on the Thermal Marangoni numbers in linear, parabolic and inverted parabolic profiles are shown in Figures (a), (b) and (c) respectively for fixed values of $Da = 10, \hat{S} = 1, \hat{T} = 1, \tau = 1, \tau_{pm} = 1,\ M_s = 10, \mu = 5.$ The line curve is for $a = 3$, the big dotted curve is for $a = 4$ and the small dotted line curve is for $a = 5$. The curves for all the profiles are converging, indicating that for larger values of depth ratios, the corresponding thermal Marangoni numbers coincide. The effect of horizontal wave number is same for all the profiles, that is the increase in the value of the horizontal wavenumber a, the value of the thermal Marangoni number increases, so the onset of double diffusive Marangoni convection is delayed and hence the system is stabilized.

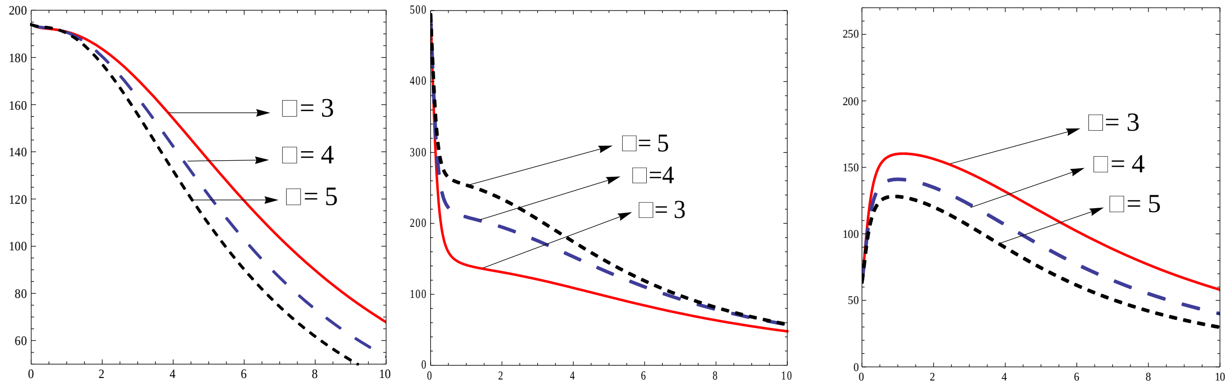

Fig. **(a)** Fig**. (b)** Fig. **(c)**

Fig.3. The effects of $\hat{\mu} = 3, 4, 5$ on the Thermal Marangoni number M_t

The effects of the viscosity ratio $\hat{\mu} = \frac{\mu_m}{\mu}$, which is the ratio of the effective viscosity of the porous medium to the fluid viscosity are displayed in Figures (a), (b) and (c) respectively for fixed values of $Da = 10, \hat{S} = 1, \hat{T} = 1,\ \tau = 1,$ $\tau_{pm} = 1, a = 5, M_s = 10.$ The line curve is for $\mu = 3$, the big dotted curve is for $\mu = 4$ and the small dotted line curve is for $\mu = 5$. The curves for the parabolic profile are converging at both the ends, (fig. 3(b)) that is, the effect of the viscosity ratio is only for the values of depth ratio $0.2 \le \hat{d} \le 10$, so the effect of the viscosity ratio is limited to this range of depth ratio. In this range, for a fixed value of depth ratio, the increase in the value of viscosity ratio $\hat{\mu} = \frac{\mu_m}{\mu}$ increases the thermal Marangoni number. Whereas the effect of the viscosity ratio is opposite to that for linear and inverted parabolic salinity profile. The curves for the linear and inverted parabolic profile are diverging and the effect of the viscosity ratio is larger for larger values of the depth ratio. For a fixed value of depth ratio, the increase in the value of viscosity ratio decreases the thermal Marangoni number and so destabilizes the system and hence the onset of the double diffusive Marangoni convection is earlier.

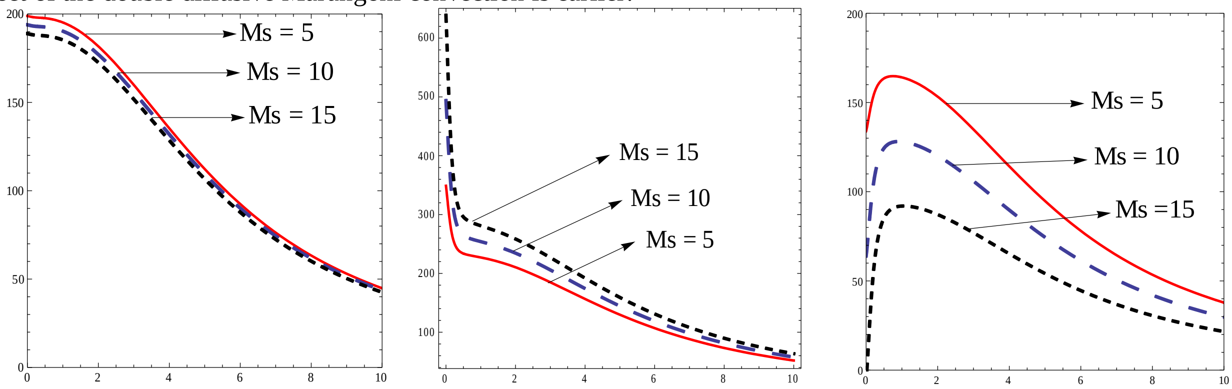

Fig. **(a)** Fig**. (b)** Fig. **(c)**

Fig.4. The effects of $M_s = 5,10,15$ on the Thermal Marangoni number M_t

The effects of the Solute Marangoni number M_s are displayed in Fig. a ,b and c for the linear, parabolic and inverted parabolic salinity profiles respectively for fixed values of $Da = 10, \hat{S} = 1, \hat{T} = 1, \tau = 1, \ \tau_{pm} = 1, a = 5, \mu = 5.$ The line curve is for $M_s = 5$, the big dotted curve is for $M_s = 10$ and the small dotted line curve is for $M_s = 15$.The curves for the parabolic profile are converging at both the ends, that is, the effect of the viscosity ratio is only for the range of values of depth ratio $1 \le \hat{d} \le 9$. The increasing values of M_s increases the value of the Thermal Marangoni number M_t i.e., to stabilize the system, so that, onset of surface driven double diffusive convection is delayed. Whereas the curves for the linear and inverted parabolic profile, are converging for larger values of depth ratio and the increase in the solute Marangoni number has no much effect of the thermal Marangoni number for larger values of the depth ratio. For a fixed value of depth ratio $\hat{d}$, the increase in the values of of the solute Marangoni number decreases the thermal Marangoni number, so the double diffusive Marangoni convection sets in earlier and hence destabilizes the system.

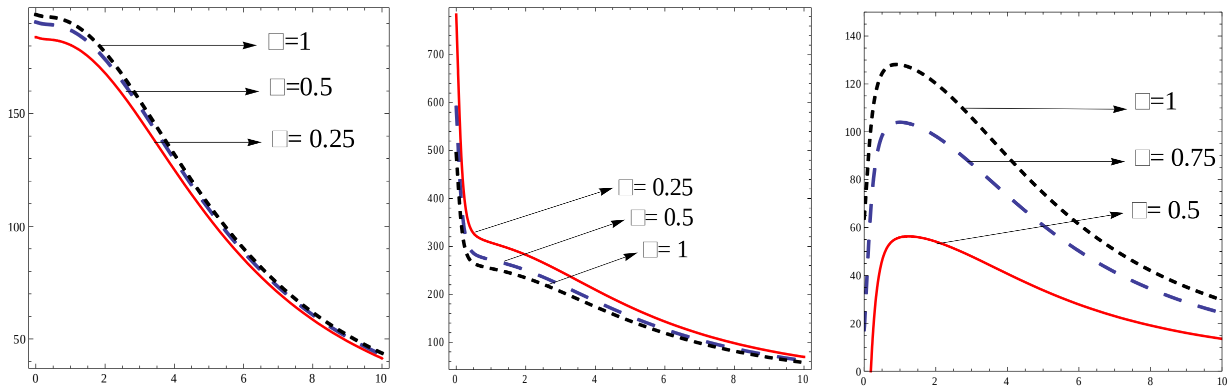

Fig. **(a)** Fig**. (b)** Fig. **(c)**

Fig.5. The effects of $\tau = 0.5, 0.75, 1$ on the Thermal Marangoni number M_t

The effects of the diffusivity ratio τ in fluid layer are displayed in Figures (a), (b) and (c) for linear, parabolic and inverted parabolic salinity profiles respectively for fixed values of $Da = 10, \hat{S} = 1, \hat{T} = 1,$ $\tau_{pm} = 1, a = 5, M_s = 10, \mu = 5.$ The line curve is for $\tau = 0.5$, the big dotted curve is for $\tau = 0.75$ and the small dotted line curve is for $\tau = 1$. The curves for the parabolic profile are converging at both the ends, that is, the effect of the viscosity ratio is only for the values of depth ratio $1 \le \hat{d} \le 10$, whereas the curves for the linear and inverted parabolic profile are converging. The increase in the values of τ increases the value of the Thermal Marangoni number M_t for the linear and inverted parabolic salinity profile, to stabilize the system, so the onset of surface driven double diffusive convection is delayed, where as the same decreases the corresponding thermal Marangoni number for the parabolic salinity profile.

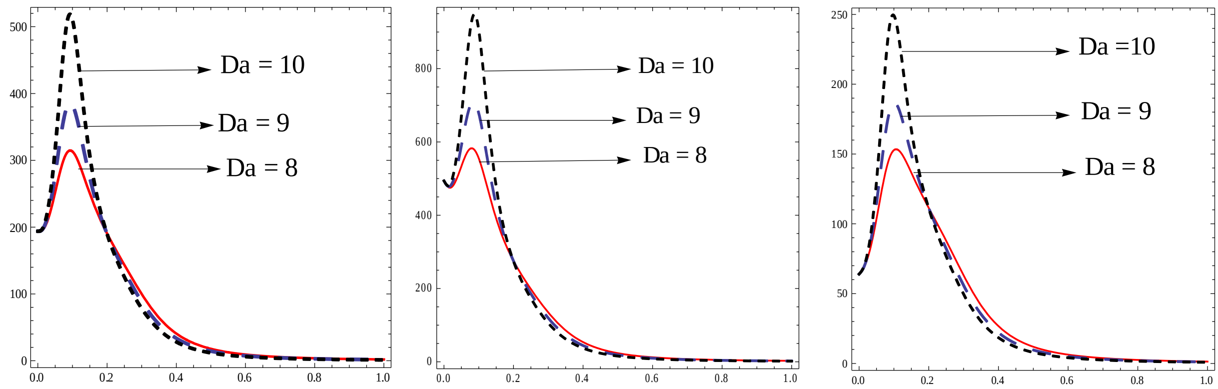

Fig. **(a)** Fig.**(b)** Fig.**(c)**

Fig.6. The effects of $Da = 8, 9, 10$ on the Thermal Marangoni number M_t

The effects of the Darcy number $Da = \beta^2 = \dfrac{K}{d_m^2}$, are displayed in Figures (a), (b) and (c) for linear, parabolic and inverted parabolic salinity profiles respectively for fixed values of $\hat{S} = 1, \hat{T} = 1, \tau = 1,$ $\tau_{pm} = 1, a = 5, M_s = 10, \mu = 5$ The line curve is for $Da = 8$, the big dotted curve is for $Da = 9$ and the small dotted line curve is for $Da = 10$. The effect of The Darcy number is visible only for small values of depth ratios. The effect of Darcy number is same for all the profiles. For a fixed value of depth ratio, increase in the value of Darcy number increases the thermal Marangoni number for all the profiles, that is this stabilizes the system, so the onset of surface driven double diffusive convection is delayed, this may be due to the presence of second diffusing component.

6. CONCLUSIONS

1. The parabolic salinity profile is the most stable one and the inverted salinity profile is the unstable one.
2. For various variations of the parameters, the effect of the parabolic salinity profile is opposite to those of linear and inverted parabolic salinity profiles except for that of Darcy number.
3. The variation of Darcy number has same effect on the onset on the double diffusive Marangoni convection for all the profiles.
4. The increase the values of horizontal wave number a, the viscosity ratio and solute Marangoni number and the decrease in the values of diffusivity ratio in the fluid layer stabilizes the system for parabolic salinity profile, where as the same destabilizes the system for the linear and inverted parabolic salinity profile.

Acknowledgements
I express my gratitude to Prof. N. Rudraiah and Prof. I.S. Shivakumara, UGC-CAS in Fluid mechanics, Bangalore University, Bangalore, for their help during the formulation of the problem.

REFERENCES

[1] I.S. Shivakumara, N. Rudraiah and C.E. Nanjundappa "Effect of non-uniform basic temperature gradients on Rayleigh-Bernad- Marangoni convection in ferrofluids" Journal of Magnetism and Magnetic Materials, 248,379-395, 2002.

[2] I.S.Shivakumara, S.Sureshkumar and Devaraju N “Effect of non-uniform temperature gradients on the onset of convection in a couple stress Fluid saturated porous medium” Journal 0f Applied Fluid Mechanics, Vol.5, No.1 , 49-55, 2012.
[3] Melviana Johnson Fu, Norihan Md. Arifin, Mohd Noor Saad and Roslinda Mohd Nazar “Effects of Non-Uniform Temperature gradient on Marangoni Convection in a Micropolar Fluid” European Journal Scientific Research, ISSN 1450-216X Vol. 28, No. 4 , 612 -620,2009.
[4] Nanjundappa Rudraiah and Pradeep G. Siddheshwar “Effect of non-uniform basic temperature gradients on the onset of Marangoni convection in a fluid with suspended particles” Aerospace science technology, 4,517-523,2000.
[5] Siti Suzillian Putri Mohamed Isa , Norihan Md. Arifin, Mohd Noor Saad and Roslinda Mohd Nazar “Effects of Non-Uniform Temperature gradient on Marangoni Convection with Free Slip Condition” Americal Journal of Scientific Research ISSN 1450-223X issue 1 , 37-44,2009.
[6] Subbarama Pranesh, Arun Kumar Narayanappa “Effect of Non-Uniform Basic Concentration Gradient on the Onset of Double-Diffusve Convection in Micropolar Fluid”, Scientific Research an academic publisher, Vol.3,No.5,May 2012.
[7] Sumithra R and Manjunath N ‘Effects of parabolic and inverted parabolic temperature profiles on magneto Marangoni convection in a composite layer’, International Journal current research(IJCR), vol.06, Issue 03, pp 5435-5450, March 2014.